J Mater Sci (2008) 43:7225–7229
DOI 10.1007/s10853-008-2945-y

Spectral and directional emittance of alumina at 823 K

George Teodorescu · Peter D. Jones

Received: 9 December 2007 / Accepted: 12 August 2008 / Published online: 17 September 2008

Abstract Spectral–directional emittance measurements of aluminum oxide (99.5% pure), in air, were performed at 823 K using an apparatus comprised of a Fourier Transform Infrared (FTIR) spectrometer, a blackbody radiating cavity (hohlraum), and a sample holder which allows directional measurements. The data cover a wide spectral range between 2 and 25 μm, and a directional range from a surface normal to a 72° polar angle. The aluminum oxide sample used in the experiment had a nominal surface roughness of 1 μm determined by a profilometer. Directional emittance shows no departure from dielectric behavior.

Introduction

Alumina (aluminum oxide) is extensively used in the ceramic industry, and alumina products are widely used in numerous fields such as chemical, petroleum engineering, natural gas, and environmental protection. Thermal management of aluminum oxide components requires knowledge of the radiative properties of aluminum oxide. Emittance is an important radiative property that facilitates not only thermal computations, but also thermography using remote sensing devices. The emittance of the opaque surface of a material is defined as:

$$\varepsilon'_{\lambda}(T,\lambda,\widehat{k}) \equiv \frac{I_{\lambda}(T,\lambda,\widehat{k})}{I_{\lambda \mathrm{b}}(T,\lambda)} \tag{1}$$

where $I_{\lambda}(T,\lambda,\widehat{k})$ is the emitted spectral intensity which leaves a surface at a specific wavelength λ and temperature T and into a direction $\widehat{k}$, and $I_{\lambda \mathrm{b}}(T,\lambda)$ is the emitted spectral intensity which leaves a blackbody at the same wavelength and temperature. Emittance is influenced by surface roughness, material composition, aging, temperature, wavelength, and direction.

The spectral normal emittance of alumina was reported in few recent studies [1–5] at different high temperatures. Vader et al. [1] report spectral normal emittance of alumina at a few high temperatures between 823 and 1593 K and for a spectral range from 1.5 to 14 μm. This is compared to data reported by Folweiler [2]. Good agreement between data reported in [1] and [2] was found except at shorter wavelengths, where the differences were attributed to the sensitivity of emittance to impurities. Brun et al. [3] report spectral normal emittance of single crystal alumina at high temperatures and determined three regions on the spectrum. Bigio [4] measured spectral normal emittance of polycrystalline alumina at wavelengths between 0.6 and 2 μm at temperatures above 1300 K and observed a slight increase in normal emittance with increasing temperature. Markham et al. [5] determined the normal emittance of sintered alumina from 1.7 to 20 μm at high temperature as the sample cools off.

All of these previous studies examined only emittance in the direction of the surface normal, and did not examine off-normal to grazing emission directions.

The purpose of this study is to determine spectral and fully directional emittance of alumina. The study examines

G. Teodorescu (✉)
275 Wilmore Laboratory, Materials Engineering Program,
Auburn University, Auburn, AL 36849-5341, USA
e-mail: teodoge@auburn.edu; teodoge@gmail.com

P. D. Jones
270 Ross Hall, Mechanical Engineering Department,
Auburn University, Auburn, AL 36849-5341, USA
e-mail: jonesp1@auburn.edu

directional emittance of alumina in order to compare and contrast with the predictions of Fresnel's relation, and to provide boundary conditions for radiative heat transfer models which are sensitive to directional data. In addition, the spectral range over which measurements are taken is made intentionally broad in order to improve its range of application. The normal emissivity of alumina at 823 K was used together with available data at the same temperature to validate the experimental setup.

Experimental apparatus

The aluminum oxide sample was mounted on a temperature-controlled heater block. The heater block and the sample are heavily insulated up to the plane of the sample surface. The heater block, the sample, and the insulation are contained in a slotted arc rack casing (Fig. 1, item 1). The sample surface temperature was monitored and controlled by a thermocouple that was embedded through the heater into the sample up to a point just beneath the sample's radiating surface. A Perkin–Elmer FTIR spectrometer (Spectrum GX) was incorporated into a previous apparatus, capable of making spectral–directional emittance measurements, which is more fully described in [6, 7].

Radiative flux is measured within a finite solid angle of 0.0049 str using a 12 mm aperture. The radiation which leaves the sample (item 2) is reflected from an off-axis parabolic gold-coated mirror (4) into a collimated beam (6). The collimated beam is then directed into an FTIR spectrometer (7) using the external FTIR spectrometer viewport. The optical path is calibrated using a blackbody (radiating cavity) which is positioned at 90° from the sample and can be viewed by rotating the gold-coated parabolic mirror. The blackbody-radiating cavity was machined into 152 mm diameter copper round stock, insulated by a 76 mm thick ceramic wool blanket, and its wall temperature was kept at the same temperature as the sample surface using a PID temperature controller. By rotating the parabolic off-axis mirror (4) using a rotation mechanism (5) and moving the sample position to a corresponding position on the slotted arc rack, measurements at different angles to the surface normal were achieved.

Measurement procedure

A 75-mm square plate of aluminum oxide (99.5% pure) with thickness of 6 mm and nominal surface roughness of 1 μm was used in the experiment. The sample surface was brought from room temperature to 823 K and maintained at 823 K for 1 h prior to taking emission measurements in order to obtain a steady state for both sample and blackbody. The radiation heat flux, which leaves the sample from an area on the plane surface, was collected by the parabolic gold-coated collector, which has a focal length of 76.2 mm. The radiation

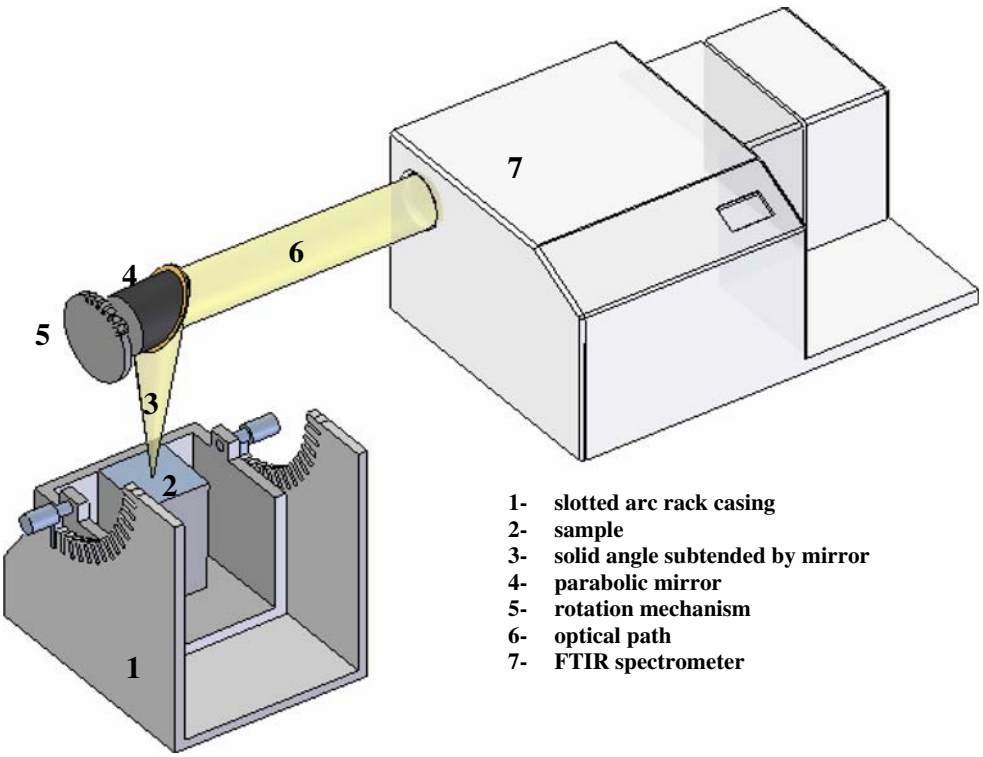

Fig. 1 Schematic of experimental setup

is then collimated by the parabolic collector into the optical path toward the FTIR spectrometer external viewport. The radiation flux was collected over a solid angle of 0.0049 str and data were averaged over ten scans using a 16 cm^{-1} resolution. The spectral–directional emittance ε is given by:

$$\varepsilon(\lambda, \theta, T_s) = \frac{I_s(T_s, \lambda, \theta) - I_b(T_r, \lambda)}{I_b(T_b, \lambda) - I_b(T_r, \lambda)} \quad (2)$$

where $I_s(T_s, \lambda, \theta)$ is the intensity emitted by the sample surface at temperature T_s, $I_b(T_b, \lambda)$ is the intensity emitted by the blackbody cavity at temperature T_b (which is equal to the sample surface at temperature T_s), and $I_b(T_r, \lambda)$ is the intensity emitted by the surrounding at room temperature, T_r. The emissivity is evaluated according to Eq. 2, taking into account the following assumptions:

1. The solid angle over which the emission signal is collected is very small, and the spectral intensity is assumed to be constant within this solid angle.
2. The blackbody cavity is perfectly black, which means that the blackbody is isothermal and its aspect ratio and aperture size produce an effective emissivity of unity.
3. The sample and blackbody surfaces are isothermal during the radiation signal measurement.
4. The broadband intensity emitted from the sample surface is unpolarized.

The uncertainty in the emittance value, $\delta\varepsilon$, is given according to [8]:

$$\delta\varepsilon_\lambda = \varepsilon_\lambda \frac{\delta T}{\lambda T_s^2} \frac{c_2}{[\exp(-c_2/\lambda T_s) - 1]} \quad (3)$$

where λ is the wavelength and c_2 is second radiation constant. According to Eq. 3, the relative uncertainty is inversely proportional to λT_s^2, resulting in a maximum uncertainty at lower temperatures and shorter wavelengths. The temperature uncertainty is comprised of the uncertainty of the blackbody temperature, sample surface temperature, and the stability of the temperature control. Uncertainties for the thermocouples and PID temperature controller used in this experiment are reported by the manufacturer to be 0.4% and 0.05%, respectively. The uncertainty estimation procedure from [8] was used to determine the total estimated uncertainty as shown in Table 1. The maximum uncertainty in the emittance value was found to be <3.5% for the spectral range considered.

The temperature of the sample surface was calculated from:

$$\frac{T_{th} - T_s}{(t/k)_{Al_2O_3}} = \mathrm{Nu}\frac{4k_a}{a}(T_s - T_a) + \varepsilon\sigma_b\left(T_s^4 - T_\infty^4\right), \quad (4)$$

where the Nusselt, Nu, number corresponds to a hot, horizontal square surface facing up [9]:

Table 1 Uncertainty Estimates of the Emissivity Measurement

Parameter	Estimated $\pm 2\sigma$ confidence limits (%)
Sample surface temperature	0.4
Blackbody temperature	0.4
Stability of the blackbody temperature	0.05
Stability of the sample temperature	0.05
Total uncertainty in emissivity $[\Sigma(\delta\mu_i)^2]^{1/2}$	0.00666
Total % uncertainty in emissivity ($\varepsilon = 0.2$, at $T = 823$ K)	3.33%

$$\mathrm{Nu} = 0.54\left[\frac{ga^3}{1/2(T_s + T_a)\nu_a\alpha_a}(T_s - T_a)\right]^{1/4}, \quad (5)$$

and where t, k, and their subscripts denote the material thickness (m) and thermal conductivity (W/m K), T_{th} and T_s are the temperature measured by the near-surface thermocouple and sample surface temperature, a is the side dimension of the square sample (m), T_a, T_∞ are the temperature of the air over the sample surface (K) and surroundings visible to sample surface, and ν_a, α_a are the kinematic viscosity of air over the sample surface (m^2/s) and the thermal diffusivity of air (m^2/s). All the thermophysical properties above were taken from data in [9] and [10], and a, $t_{Al_2O_3}$ were measured. T_a and T_∞ were taken to be equal and T_{th} is recorded from each experiment setup. In practice, T_s was determined to be 5° lower than T_{th}.

Results and discussion

The measured normal emittance of alumina is shown in Fig. 2 together with data published by Vader et al. [1]. The data represent an average of three measurements of ten scans with a resolution of 16 cm^{-1}, each collected at different times. The spectral normal emittance from the present work shows good agreement with reported data from [1] at a temperature of 823 K and for a spectral range from 2 to 14 μm. Differences within uncertainty limits are seen in spectral range from 12 to 14 μm, and we attribute these to differences in sample surface roughness, although the sample surface roughness in [1] was not reported.

Figure 3 presents the normal emittance of aluminum oxide at 823 K measured in the present work for a wider spectral range, up to 25 μm. Typically, the spectral normal emittance of a dielectric metallic oxide like Al_2O_3 has three different regions, according to Brun et al. [3]: a transparency region from the visible part of the spectrum to around 3 μm, a multiphonon or semitransparent region typically from 3 μm up to around 10 μm, where a maximum emittance is exhibited, and a phonon or opaque region beyond

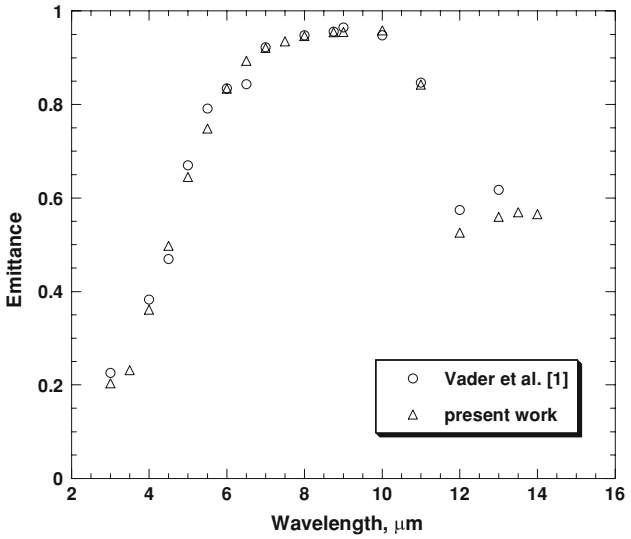

Fig. 2 Spectral normal emittance of Al_2O_3 at 823 K. Comparison between present work and data reported by Vader et al. [1]

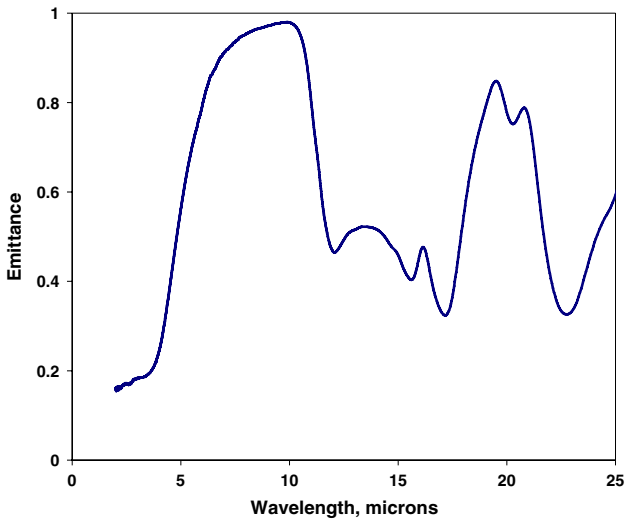

Fig. 3 Measured spectral normal emittance of alumina at 823 K

the maximum value in emittance. Both semitransparent and opaque regions of aluminum oxide are illustrated in [3] and in the present work as shown in Figs. 2 and 3.

The measured normal emittance shows a maximum (Christiansen's point) in emittance around 10 μm, similar to that obtained by [2, 3]. At Christiansen's point (wavelength) a heteropolar oxide behaves as a blackbody [3]. The directional emittance of alumina measured in the present work is tabulated in Table 2. The polar angles considered range between the normal to the sample surface and 72° (near grazing) with a step increment of 12°. A characteristic dielectric directional behavior derived from Fresnel's equation is represented in Fig. 4 for a refractive index, $n = 5.5$ and an extinction coefficient, $k = 0$.

Table 2 Measured spectral–directional emittance of alumina at 823 K

λ, μm	Polar angle, deg						
	0°	12°	24°	36°	48°	60°	72°
2	0.156	0.156	0.156	0.151	0.139	0.130	0.118
3	0.184	0.184	0.184	0.174	0.172	0.164	0.151
4	0.244	0.244	0.244	0.237	0.231	0.222	0.205
5	0.562	0.562	0.562	0.553	0.539	0.523	0.469
6	0.796	0.796	0.796	0.789	0.772	0.751	0.671
7	0.912	0.912	0.912	0.906	0.891	0.867	0.776
8	0.953	0.953	0.953	0.948	0.936	0.912	0.824
9	0.971	0.971	0.971	0.968	0.958	0.938	0.854
10	0.979	0.979	0.979	0.977	0.968	0.945	0.840
11	0.801	0.801	0.801	0.723	0.628	0.506	0.488
12	0.466	0.466	0.466	0.450	0.434	0.353	0.411
13	0.515	0.515	0.515	0.507	0.502	0.436	0.480
14	0.516	0.516	0.516	0.512	0.514	0.464	0.509
15	0.459	0.459	0.459	0.456	0.465	0.422	0.488
16	0.461	0.461	0.461	0.457	0.469	0.433	0.510
17	0.332	0.332	0.332	0.329	0.352	0.324	0.443
18	0.535	0.535	0.535	0.533	0.550	0.545	0.632
19	0.782	0.782	0.782	0.777	0.776	0.757	0.761
20	0.777	0.777	0.777	0.772	0.767	0.732	0.722
21	0.766	0.766	0.766	0.759	0.747	0.705	0.699
22	0.406	0.406	0.406	0.404	0.416	0.387	0.500
23	0.332	0.332	0.332	0.332	0.356	0.342	0.497
24	0.478	0.478	0.478	0.479	0.487	0.501	0.624
25	0.593	0.593	0.593	0.612	0.601	0.617	0.707

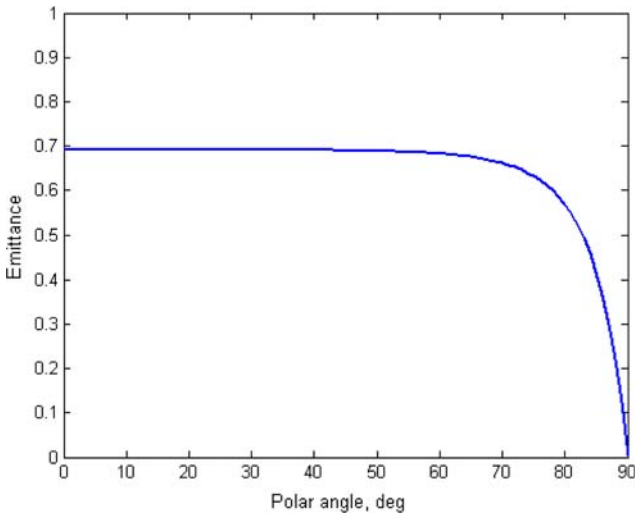

Fig. 4 Directional emittance of a dielectric

Directional emittance of an optically smooth dielectric is described by Fresnel's relation, and also follows Lambert's law from angles normal to the sample surface to

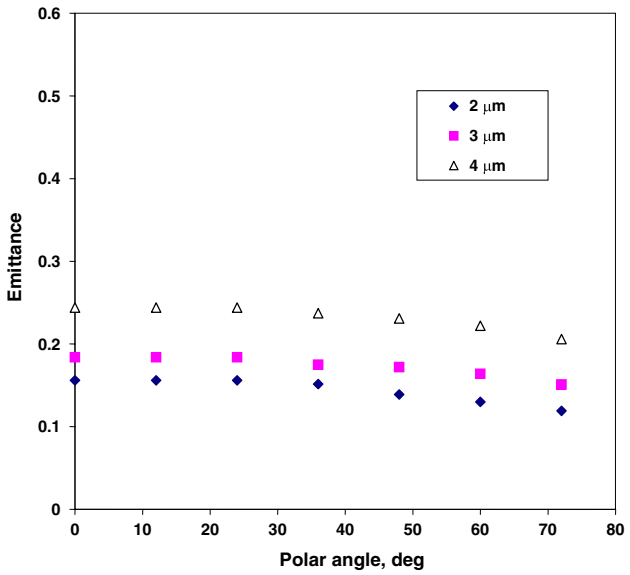

Fig. 5 Measured directional emittance of alumina at 2, 3, and 4 μm

typically 50–60° before a sudden decrease to zero [10]. The Fresnel's equation described in Eq. 6 assumes that the vacuum to material interface is sharp and the optical properties n and k are constant with depth into the material. The equation also assumes an isotropic material with no dependence on the azimuthal angle.

$$\varepsilon_\lambda = 1 - \frac{1}{2}\left(\frac{(n_\lambda\beta - \cos\theta)^2 + (n_\lambda^2 + k_\lambda^2)\alpha - n_\lambda^2\beta^2}{(n_\lambda\beta + \cos\theta)^2 + (n_\lambda^2 + k_\lambda^2)\alpha - n_\lambda^2\beta^2} + \frac{\left(n_\lambda\gamma - \frac{\alpha}{\cos\theta}\right)^2 + (n_\lambda^2 + k_\lambda^2)\alpha - n_\lambda^2\gamma^2}{\left(n_\lambda\gamma + \frac{\alpha}{\cos\theta}\right)^2 + (n_\lambda^2 + k_\lambda^2)\alpha - n_\lambda^2\gamma^2}\right) \quad (6)$$

where

$$\alpha^2 = \left(1 + \frac{\sin^2\theta}{n_\lambda^2 + k_\lambda^2}\right)^2 - \frac{4n_\lambda^2}{n_\lambda^2 + k_\lambda^2}\left(\frac{\sin^2\theta}{n_\lambda^2 + k_\lambda^2}\right), \quad (7)$$

$$\beta^2 = \frac{n_\lambda^2 + k_\lambda^2}{2n_\lambda^2}\left(\frac{n_\lambda^2 - k_\lambda^2}{n_\lambda^2 + k_\lambda^2} - \frac{\sin^2\theta}{n_\lambda^2 + k_\lambda^2} + \alpha\right), \quad (8)$$

$$\gamma = \frac{n_\lambda^2 - k_\lambda^2}{n_\lambda^2 + k_\lambda^2}\beta + \frac{2n_\lambda k_\lambda}{n_\lambda^2 + k_\lambda^2}\left(\frac{n_\lambda^2 + k_\lambda^2}{n_\lambda^2}\alpha - \beta^2\right)^{\frac{1}{2}}, \quad (9)$$

The spectral–directional emittance data with a wavelength step increment of 0.5 μm are presented in Table 2. Directional emittance of alumina at wavelengths of 2, 3, and 4 μm shown in Fig. 5, follows Lambert's law from angles normal to the sample surface up to 48° before diving to zero at grazing angles according to Fresnel's relation for a dielectric material [10]. Based on directional emittance determined, alumina follows a dielectric behavior.

Conclusions

Spectral emittance of polycrystalline alumina with known surface roughness was measured at 823 K with an experimental setup which allows fully directional measurements. A broad spectrum from 2 to 25 μm is achieved by using an FTIR spectrometer. The normal emittance of alumina shows very good agreement with reported data [1] over a spectral range from 2 to 14 μm and a maximum in alumina emittance was found at a wavelength around 10 μm similar to that reported in [2] and [3]. Directional emittance shows no departure from dielectric behavior.

References

1. Vader DT, Viskanta R, Incropera FP (1985) Rev Sci Instrum 57(1):87. doi:10.1063/1.1139125
2. Folweiler RC (1962) USAF technical document report no. ASD-TDR-62-719. U.S. GPO, Washington, D.C., USA
3. Brun JF, De Sousa Meneses D, Echegut P (2003) In: Paper presented at 15th symposium of thermophysical properties, June, Boulder, CO, USA
4. Bigio L (1999) GE technical document report no. 99. CRD128, U.S. Research and Development
5. Randolph CP, Overholzer MJ (1913) Phys Rev 2:144. doi: 10.1103/PhysRev.2.144
6. Jones PD, Dorai-Raj DE, Mcleod DG (1996) J Therm Heat Trans 10(2):343. doi:10.2514/3.793
7. Jones PD, Teodorescu G, Overfelt RA (2006) J Heat Transfer 128:382. doi:10.1115/1.2165207
8. Teodorescu G, Jones PD, Overfelt RA, Guo B (2006) Int J Thermophys 27(2):554. doi:10.1007/s10765-005-0009-y
9. Incropera FP, Dewitt DP (2002) Fundamentals of heat and mass transfer, vol 5. Wiley, New York
10. Modest MF (2003) Radiative heat transfer, 2nd edn. Academic Press, New York